Machine vision analysis of the energy efficiency of intermodal freight trains

Y-C Lai[1]*, C P L Barkan[1], J Drapa[1‡], N Ahuja[2], J M Hart[2], P J Narayanan[3], C V Jawahar[3], A Kumar[3], L R Milhon[4], and M P Stehly[5]

[1]Railroad Engineering Program, University of Illinois at Urbana-Champaign, Newmark Civil Engineering Laboratory, Urbana, Illinois, USA

[2]Computer Vision and Robotics Laboratory, University of Illinois at Urbana-Champaign, Beckman Institute, Urbana, Illinois, USA

[3]Centre for Visual Information Technology, International Institute of Information Technology, Gachibowli, Hyderbad, India

[4]Technical Research and Development, BNSF Railway, Topeka, Kansas, USA

[5]Environment and Research Development, BNSF Railway, Fort Worth, Texas, USA

Abstract: Intermodal (IM) trains are typically the fastest freight trains operated in North America. The aerodynamic characteristics of many of these trains are often relatively poor resulting in high fuel consumption. However, considerable variation in fuel efficiency is possible depending on how the loads are placed on railcars in the train. Consequently, substantial potential fuel savings are possible if more attention is paid to the loading configuration of trains.

A wayside machine vision (MV) system was developed to automatically scan passing IM trains and assess their aerodynamic efficiency. MV algorithms are used to analyse these images, detect and measure gaps between loads. In order to make use of the data, a scoring system was developed based on two attributes – the aerodynamic coefficient and slot efficiency. The aerodynamic coefficient is calculated using the Aerodynamic Subroutine of the train energy model. Slot efficiency represents the difference between the actual and ideal loading configuration given the particular set of railcars in the train. This system can provide IM terminal managers feedback on loading performance for trains and be integrated into the software support systems used for loading assignment.

Keywords: environment, energy efficiency, aerodynamics, fuel use, intermodal, machine vision, image analysis algorithms

1 INTRODUCTION

Energy cost has long been recognized as an important factor in railway operating efficiency [1]. In 2005, the major North American railroads spent over $8 billion on fuel in the US making it their second largest operating expense [2] and fuel cost continues to increase (from 2002 to 2005, North American railroad fuel cost doubled, and since 1999 it is up by nearly a factor of 3). This trend is impacting railroads all over the world, consequently, fuel efficiency is more important than ever [3–5]. The sharp increase in energy costs, combined with railways' growing interest in improving their role as an environmentally sustainable transport mode has stimulated renewed interest in research on all aspects of energy efficiency [6, 7]. This includes investigation of technologies to improve the efficiency of motive power, recover kinetic energy

---

Corresponding author: Department of Civil and Environmental Engineering, University of Illinois at Urbana-Champaign, B118 Newmark Laboratory, 205 North Mathews Avenue, Urbana, IL 61801, USA. email: lai3@uiuc.edu

‡Now at: Transportation Technology Center, Inc., 55500 DOT Road, PO Box 11130, Pueblo, CO 81001, USA.

of moving trains, energy efficient design of railway vehicles, more efficient operations, prevention of fuel spillage, and various approaches to reduce train resistance [**3**, **5**, **8**].

The current paper describes research on the reduction of train resistance and focuses on a particularly important segment of North American railroad freight transportation, intermodal (IM) trains [**2**, **9**]. Railroads are the largest transporter of intercity freight in North America, and in 2003, despite continued growth in coal traffic, IM traffic surpassed it as the leading source of US railroad freight revenue for the first time in history [**2**]. This dramatic growth in IM traffic means that it is having an increasing impact on operating costs, and fuel is the second largest of these, comprising approximately 12 per cent of US railroads' total in 2004 [**2**]. It is ironic that at a time of rapidly increasing energy costs, the largest segment of freight traffic growth, namely IM, is also the least energy efficient. Because of constraints imposed by the design and diversity of equipment, IM trains incur greater aerodynamic penalties and increased fuel consumption compared to their general freight counterparts. In order to compete effectively with highway transport, IM trains are typically the fastest freight trains operated thereby amplifying the effect of their poor aerodynamics. The profit margin on IM freight is often low, making it particularly sensitive to price and service competition from trucks [**9**, **10**]. Consequently research to understand and reduce IM train resistance is important, both to reduce fuel costs so as to sustain a competitive cost structure and to minimize the environmental impact resulting from the high-speed requirements needed to sustain and grow this traffic.

Although energy efficiency has always been an important focus of railways, the sharp increase in petroleum costs that occurred in 1970s stimulated new research on the subject. Among the studies that resulted were investigations of technologies to reduce train resistance and thereby improve efficiency [**11–14**]. Aerodynamic drag has long been known to be a major component of the total train resistance, particularly, at higher speeds [**15**], so the Association of American Railroads (AAR) supported research on wind tunnel testing of rail equipment, including large-scale IM car models [**16–19**]. The results were used to develop the Aerodynamic Subroutine of the AAR's train energy model (TEM) [**20**].

More recently, it has been shown that the pattern of IM equipment loading affects resistance and that it can be reduced through certain operational changes. Lai and Barkan [**21**] conducted a series of analyses to compare both the relative and absolute effects of different loading patterns and operating practices on train make-up and energy efficiency. They found that aerodynamic characteristics significantly affect IM train fuel efficiency. Trains can be more efficiently

operated if loads are assigned to each available space on IM cars and further improvement is possible if the gaps between loads are minimized.

The substantial energy savings that may be accrued due to improved loading patterns suggested the potential benefit of a system to monitor IM train loading. Consequently, a wayside machine vision (MV) system was developed to automatically scan passing trains and assess the aerodynamic efficiency of their loading patterns. A digital video recording system is used to record passing trains, and MV algorithms analyse the images to detect and identify loads, and to measure the gaps. After recording a train, the video is processed and histograms of gaps are generated to represent the loading pattern of the train. In order to make use of the data, a scoring system is also proposed to compare the actual configuration to the ideal configuration, thereby providing feedback to terminal managers on how well trains are being loaded.

In the current paper, sections 1 to 3 summarize the analyses of loading efficiency of IM trains. Section 4 describes the automated wayside MV system to monitor IM train loading patterns, and section 5 describes the scoring system to provide a metric of IM train loading efficiency.

1.1 Loading assignment at IM terminals

At IM terminals, containers or trailers are assigned to available well, spine or flat cars [**22**, **23**]. The standard length of IM loads (i.e. trailers or containers), transported on North American railroads are 20, 28, 40, 45, 48, 53, and 57 ft (6.1, 8.5, 12.2, 13.7, 14.6, 16.2, and 17.4 m) [**2**, **6**, **10**, **24**]. There is considerable variety in the design and capacity of IM railcars including variability in the number of units and slots, and thus loading capabilities; however, they can be broadly classified into three basic type flat cars, spine cars, and well cars (Fig. 1). IM railcars may be a single unit, or can have up to five permanently connected units (via
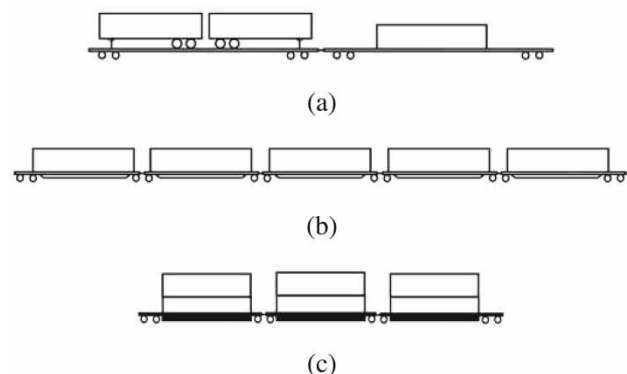

Fig. 1   (a) A 2-unit flat car; (b) a 5-unit spine car with five slots; and (c) a 3-unit well car with six slots

articulation or drawbar). A unit is a frame supported by two trucks (bogies), providing support for one or more platforms (also known as slots). For example, Fig. 1(a) depicts a 2-unit flat car, Fig. 1(b) a 5-unit spine car, and Fig. 1(c) an articulated 3-unit well car specially designed to 'double-stack' containers, thereby doubling their capacity without substantial lengthening of the train. Flat and spine cars transport both trailers and containers but well cars typically transport only containers. The term 'well' refers to the depressed centre section slung between the trucks that provide a low platform that enables one container to be stacked atop another and still remain within the clearance limits of many North American rail lines. A platform (or slot) is a specific container or trailer loading location. Most units have a single slot; however, well-car units have two slots because of their ability to hold two or more containers.

Loading rules regarding feasible and infeasible combinations of IM loads and railcars have been developed to ensure safe and efficient operation. Terminal managers often use computer software [25] tools to aid them in complying with these loading rules; however, load assignment is still a largely manual process. Operating efficiency is enhanced if trains operate with as many slots filled as possible. Railroads have developed a metric to measure the efficiency of loading, which is termed, 'slot utilization' [26]. Although the details vary depending upon the particular combination of IM load and car being considered, slot utilization is basically a measurement of the percentage of available slots that are used for loads. Slot utilization does not take into account the size of the slot compared to the size of the load. Although perfect slot utilization indicates maximal use of the feasible slots available, it is not intended to, nor does it ensure, that IM cars are loaded to maximize the energy efficient operation of IM trains. Two trains may have identical slot utilization, but different loading patterns and consequent train resistances [21].

Improving the loading patterns of IM trains has the potential to improve railroad fuel efficiency and reduce emissions. Maximizing slot utilization improves energy efficiency, but matching IM loads with appropriate length IM car slots reduces both excess weight, and gap length between loads, and thereby reduces train resistance.

2 METHODOLOGY

The aerodynamic coefficient, train resistance, and estimated fuel consumption were used to compare the energy efficiency of different loading patterns using the Aerodynamic Subroutine [27] and TEM [20]. Train

resistance is the sum of the forces opposing the movement of a train [28]. The greater the resistance, the more energy is required to move the train.

The resistance equation in this study is derived from the general expression, which can be represented as [28, 29]

$$R = R_{Bk} + R_{Rk} + CV^2 \qquad (1)$$

A more detailed derivation of this model is presented and discussed in reference [21]. The term C can be computed from Aerodynamic Subroutine by specifying a train consist. The aerodynamic coefficient is also affected by wind direction. However, since the analysis is intended to be generic for trains operating anywhere at anytime, incorporation of a wind direction coefficient would be inappropriate. A detailed analysis of a specific route might require that this factor be incorporated if the route had strong and consistent prevailing winds. Bearing and rolling resistance are related to train weight and are computed using the equations in TEM [20].

3 MATCHING IM LOADS WITH CARS

Capacity of IM cars is usually constrained by the length of the slot. For example, a 5-unit, articulated, double stack well car with a 40-ft well cannot handle containers greater than this length in the bottom position, whereas a 5-unit car with a 48-ft well can handle containers up to 48 ft in length [22–24, 30]. Consequently, cars with longer wells are more flexible; however, if they are loaded with containers shorter than the maximum they allow, the gaps between loads are correspondingly larger, and therefore less aerodynamically efficient.

Previous research [21] has shown a strong, positive relationship between gap length and aerodynamic coefficient for gap lengths up to 12 ft (3.66 m) (Fig. 2).
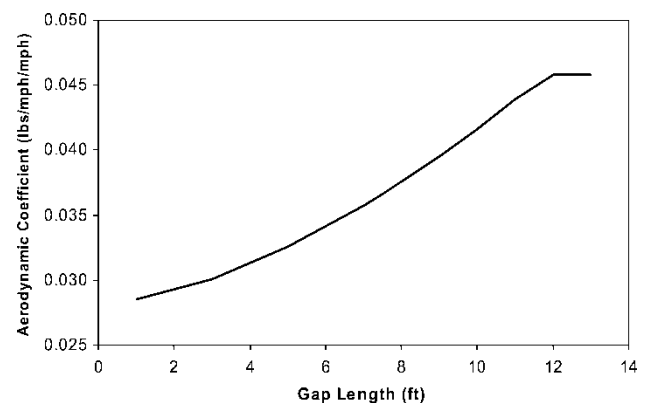

Fig. 2 Critical gap length of well cars

For gaps greater than 12 ft (3.66 m), there is no additional effect [16] and this is referred to as 'critical gap length'.

3.1 Aerodynamic coefficient and train resistance

The most common IM loading combinations observed in this study were double-stack containers in well cars, trailers on spine cars, and containers on spine cars. Although flat cars are also part of the IM fleet, their use is declining and their characteristics are similar to spine cars. Therefore, efficiency analyses were conducted on the first two scenarios: (a) matching double-stack containers on well cars and (b) matching trailers on spine cars. The effect of matching containers on spine cars is intermediate between its effect on double-stack well cars and trailers on spine cars [21].

A train of three locomotives and 100 units (20 five-unit cars) was chosen as suitably representative for this analysis. A 40-ft container can be assigned to a car with 40-ft, 48-ft or 53-ft wells; however, use of a car with 40-ft wells would result in the shortest gap length and the best aerodynamics.

For a train of 20 cars with 40-ft double stack containers, the aerodynamic coefficient increases from 4.82 to 5.05 lbs/(mile/h)^2 (0.855 to 0.895 kg/(km/h)^2) when 48-ft or 53-ft-well cars are used instead of 40-ft. Using either 48-ft or 53-ft-well cars results in similar aerodynamic resistance because the gap lengths in both cases are greater than the critical gap length.

The total train resistance was calculated for these three train configurations for speeds up to 70 mile/h. As expected the train with 40-ft-well cars had the lowest resistance at all speeds (Fig. 3(a)). The train with 48-ft-well cars had higher resistance mainly because of the aerodynamic penalty, but also due to the heavier weight of the longer car. The train with 53-ft-well cars experienced the same aerodynamic penalty as

the 48-ft-well cars because the gaps for both cars were greater than the critical gap length. However, the 53-ft car had an additional, 34 per cent higher weight penalty, and correspondingly, greater bearing resistance [24]. The increase in lightweight between the 48-ft and 53-ft-well cars is not proportional to the increase in length because the 53-ft-well cars are also designed for greater weight capacity and thus are more robustly constructed [30].

Compared to 40-ft double stack containers on cars with 40-ft wells, transporting 40-ft containers on 48-ft-well cars would consume 12.6 gallons (47.70 l) more fuel per train per 100 miles (160.93 km) compared to use of 40-ft-well cars, mainly due to the aerodynamic effect. The weight penalty for a train travelling the same distance with the same loads on 53-ft-well cars would require an additional 40 gallons (151.42 l) of fuel per train. The estimated fuel savings in these two examples ranges from 0.13 to 0.52 gal/mile (0.306 to 1.223 l/km), respectively.

Similarly, a 48-ft trailer can be assigned to a spine car with 48-ft, or 53-ft wells, but choosing 48-ft-slot spine car should be more efficient. For a train of 20 spine cars with 48-ft trailers, the aerodynamic coefficient increases from 5.90 to 9.12 lbs/(mile/h)^2 (1.046 to 1.617 kg/(km/h)^2) when 53-ft-slot cars are used instead of 48-ft-slot cars. The difference in resistance ranges from 0.07 to 26.72 per cent depending on speed (Fig. 3(b)), and the difference in fuel consumption on the example route is estimated to be more than 1 gal/mile (2.351 l/km).

In summary, matching IM loads with cars reduces train resistance and fuel consumption. In the case of well cars, there is less reduction in aerodynamic resistance but more reduction in bearing resistance, whereas for spine cars the reduction in resistance is primarily due to the improved aerodynamics that are possible if loads are properly matched with cars.
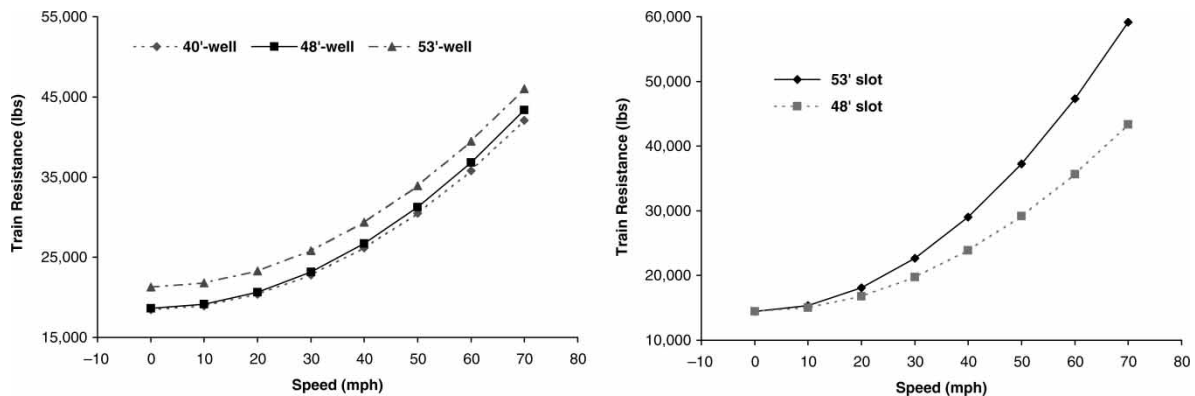

Fig. 3 Train resistances of (a) double-stack 40-ft containers on 40-ft, 48-ft, or 53-ft well cars (b) trailers on 48-ft-slot, or 53-ft-slot spine cars

4 WAYSIDE MV SYSTEM

The substantial energy savings possible from improved loading patterns suggested that a system to monitor IM train loading could be beneficial. Consequently, the BNSF Railway undertook development of an automated, wayside, MV system to record and analyse the loading patterns of IM trains. The system enables automatic monitoring of trains to determine their efficiency by analysing load type, railcar type, matching, and position in the train. This system provides feedback on specific trains originating from particular terminals to help managers build and dispatch more efficiently loaded trains. It also enables BNSF to assess the loading efficiency of trains it receives in exchange from other railroads.

The first step is to record a digital video of trains passing by a wayside camera and computer installation. MV algorithms detect the IM loads on each individual car-unit in the train and identify their type, size, position, and the gaps between the IM loads. From these data, loading efficiency is determined based on the gaps present compared to ideal loading configurations for the particular type of railcars in the train.

4.1 Image acquisition system

An initial, portable MV image acquisition system was developed to acquire videos of passing trains from wayside locations. It consists of the video camera and lens, laptop computer, and imaging software. A Sony DFW-V500 digital video camera with a 1/2 in (1.27 cm) colour CCD sensor captures video in non-compressed YUV format and transfers it to a computer via a FireWire 1394 serial bus at 30 frames per second, saving it in AVI format. A Tamron lens with low aspheric distortion, a variable focal length of 6–12 mm, and an f-stop of 1.0 for low lighting conditions is used. The camera is rotated 90° to provide a larger vertical field of view for capturing the full, 20 ft (6.10 m) height of loaded double stack cars which are the tallest rail equipment typically operated on North American railroads.

The portable MV system was tested at two locations on the Chillicothe Subdivision of the BNSF Railway's Chicago Division; near Coal City, Illinois (MP 54.7), and just outside of Streator, Illinois (MP 77). This is the BNSF's principal route for transcontinental IM traffic and sees upward of 50 IM trains per day often travelling at speeds as high as 70 mile/h (112.65 (km/h)). Therefore, it was a good location to obtain a large amount of data on IM trains with a variety of load configurations. Principal testing of the system was at the Coal City location because the double track main line is spaced far enough apart to allow video recording of trains on either track from a location between the two. This also eliminates the possibility of having another train to move behind the subject train, which would confound the current MV algorithms for identifying IM loads. A substantial library of videos including a wide range of IM car and load combinations was collected and used to develop and test the MV algorithms.

A permanent, automated wayside version of this system has recently been installed at the BNSF Railway's Logistics Park – Chicago IM facility (known as LPC). This installation features hardened components housed in an equipment bungalow and on two towers (Fig. 4). The camera is installed on one of the towers inside a weatherproof housing. The other tower provides an antenna for communication with the main LPC yard office. This connection allows data to be transmitted directly to BNSF's computer system for analysis. The LPC installation is fully automated. Wheel detectors on either side of the wayside system detect the arrival of a train and trigger the onset of video capture; and an automatic equipment identification (AEI) system reads the tags on the cars as the train passes. The video is then processed by the MV algorithms, followed by data analysis and reporting to BNSF.

4.2 Overview of MV algorithms

There are several steps involved in detecting and extracting relevant information from the digital video generated from the image acquisition system. First, the software separates the image of the train from the background in each frame. The frames, with the unwanted background information removed, are then analysed using a velocity estimation module that enables the patching of consecutive frames to produce a panoramic image of the entire train. Edge-detection algorithms, along with the prior information regarding the loading patterns, are used in the next stage to make intelligent inferences concerning the location
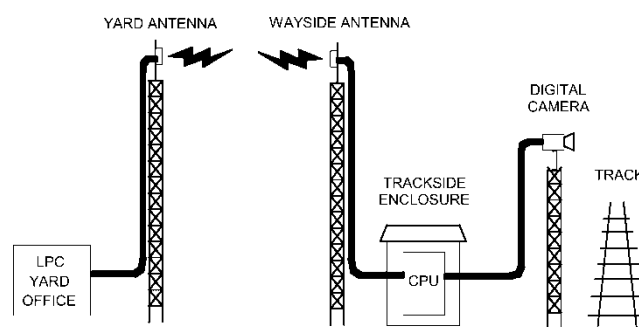

Fig. 4 Conceptual diagram depicting the principal elements of the automated, wayside image acquisition system as installed at LPC

of the containers and the gaps between them. Certain distinguishing characteristic patterns of trailers and containers are used to determine the location and type of loads. Information regarding the identification, location, and spacing of IM loads is then analysed and summarized and several diagnostic statistics are generated using separate software modules.

4.2.1   Separating the train from the background

In order to more easily process the train video using MV algorithms, the background area is removed from the video frames primarily leaving the train in the image. The initial algorithm functioned if the background was fairly stable during the time it took for a train to pass by. Thus a simple template-based background subtraction was used in which the background was recorded before the arrival of the train. When the train arrived in the field of view, its image was captured and the background template subtracted, thereby largely removing it. However, subtle changes in the background, such as movement of clouds or wind-induced motion of trees, sometimes caused problems in the subtraction routine that confounded later stages of the algorithm and reduced its reliability in properly detecting IM loads. Consequently, a more complex method using a probabilistic learning algorithm was developed (Fig. 5). This method used the initial part of the video, before the train appears, to model the variation in the background pixels and then learn which pixel intensities are in the background, and which are in the foreground. However, this sometimes led to erroneous classification of pixels since the colour of the background was often the same as the colour of the loads. Therefore, the resulting background subtraction was still not satisfactory. Up to this point, prior knowledge of the shape of the loads had not been used to help distinguish the foreground from the background. This information is easily available at the boundaries of loads, which are often either horizontal, such as the top edge of a load, or vertical as in the side edge of a load. It was found that use of edge detection of loads is robust and is not confounded by other
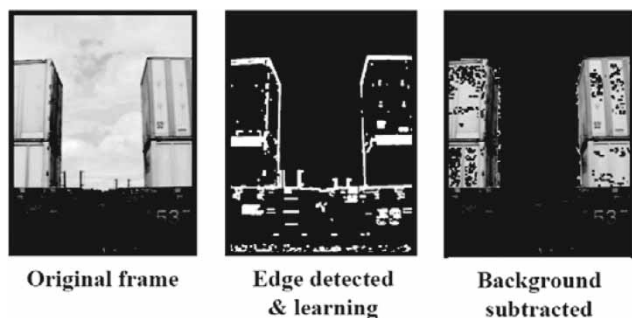

Original frame   Edge detected & learning   Background subtracted

Fig. 5   Background subtraction module extracts the train and separates it from the background

edges in the background. Integrating this with the learning algorithm described above achieves nearly complete background subtraction for each frame, thus increasing the accuracy of load edge detection.

4.2.2   Continual estimation of train velocity

The velocity is calculated between consecutive images in the video (Fig. 6(a)). It is computed by finding the best correlation shifts for all three-colour signals in the adjacent foreground extracted (train pixels only) frames. These colour signals are the integral of all the colour energy found in a strip of prescribed vertical columns whose centre is chosen as the centre column of each frame. The correlations can be used to calculate the sum of squared error at various pixel shifts. The lowest error value gives the pixel shift that best estimates the velocity of the train. The central pieces of the frames with the background removed, are then pieced together (Fig. 6(b)). The mid-section of each frame in the video is used to construct the panorama because the centre of the lens produces the least distortion. It is concatenated to the existing panorama based on its pixel velocity relative to the previous frame. This method differs from normal panoramic image generation, which is constructed by piecing together images taken while moving the camera location. The approach developed in this research utilizes the movement of the train and the consecutive video frames to create a panorama of the entire train with a single camera position (Fig. 6(c)).

### 4.2.3   Detection of edges and load identification

The loads on the train and their loading pattern are then processed from the constructed panorama. The algorithm follows a decision tree path in which it first determines if a particular location has a gap or a train object. If the lack of a gap is determined due to train pixels being present in the area of the panoramic image, it then proceeds to find the top horizontal edge of the load and creates a simple vertical projection of colour intensities and uses this projection to distinguish the difference between a trailer and a container. The height is then checked on the load identified to determine if it is a single container, double-stacked containers, or a trailer. If so, the system finds the dividing line between the upper and lower containers and then their individual vertical boundaries in order to establish their individual sizes.

4.2.4   Gap estimation and measurement

The gap is measured by the homography that is initially calculated from the camera parameters and a training image. This allows the program to determine the distance in real world measurement units as long as the
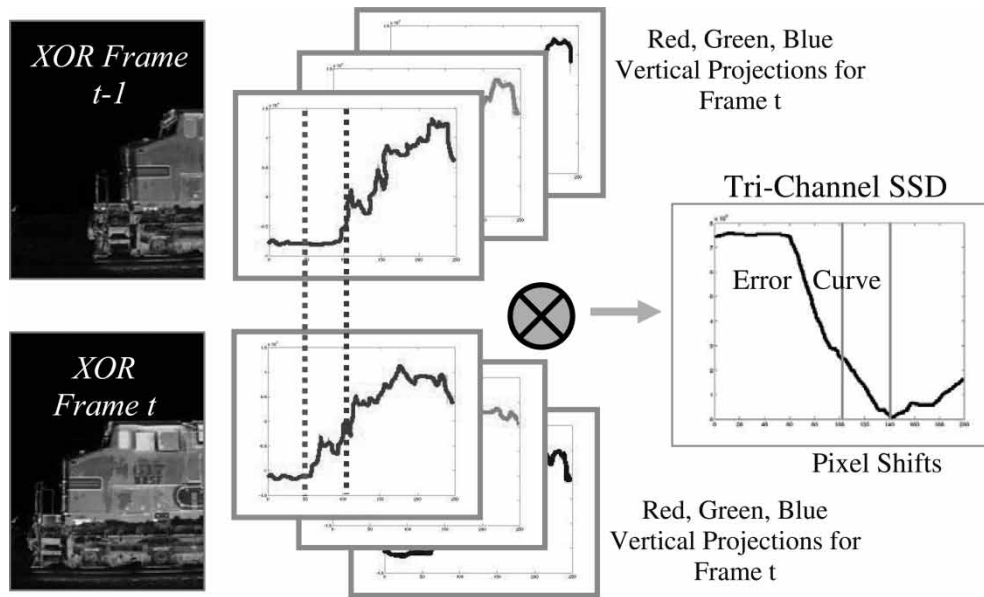
(a)
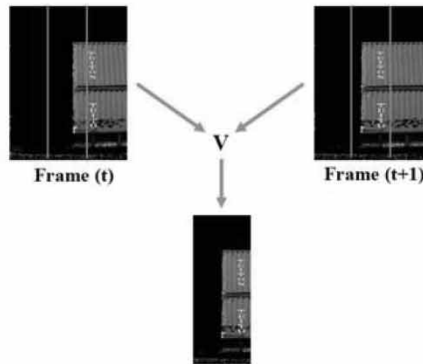
(b)

(c)

Fig. 6 (a) Velocity estimation; (b) assembling the centre sections of consecutive frame to form the panoramic image; and (c) example panoramic image of part of a train cut into multiple pieces for image display purposes

Fig. 7 Detection of gap boundaries (marked in blue) and identification of the object between the gap edges (marked with a red boundary to indicate a container)

pixels that are being visualized are on the plain formed by the loads and/or side of the train that the camera images. The vertical edges are colour-coded in blue, the horizontal edges of containers in red, and trailers in green. Once the blue gap lines are determined in the images (Fig. 7), the distance between two consecutive blue lines that do not have a load object between them gives the gap length in pixels. These units are then homographically converted into a measurement of gap length measured in feet as described above.

4.3 Loading pattern monitoring

After recording a train, the video is processed and histograms of upper and lower gaps are generated to represent the loading pattern of the train. This information is necessary but not sufficient to evaluate the efficiency of loading patterns. In order to make use of the data, a scoring system is used to compare the actual configuration to the ideal configuration.

4.3.1 Gap histogram

For typical flat and spine cars, there are only gaps at one level; however, for well cars, a histogram is needed for both levels due to the double stacking of loads. An upper level gap is the gap between two upper level containers, which exists whenever there are at least two double-stacked containers in the train. Similarly, a lower level gap is the gap between two lower level loads (Fig. 8).

The histograms provide an easy-to-interpret visual depiction of the frequency distribution of gap length for each train (Fig. 9). The loading pattern of the train

represented in Fig. 9 is not very efficient as evidenced by the large number of gaps greater than 12 ft (3.66 m), and several very large gaps in the upper level. The slope of the cumulative percentage gives the user further information; the steeper the slope the better the efficiency, because it indicates a larger percentage of short gaps.

4.3.2 System validation

To evaluate the accuracy of the MV system, the actual length and distribution of gaps was manually determined by viewing and measuring the gaps recorded on the digital train videos, and comparing the results to what the MV algorithms calculated for the same videos. Two types of errors may occur in gap-length detection.

1. Edge detection error in which the system does not precisely detect the edges of the load because of background elimination problems or some object such as a refrigeration unit mounted on the end of loads that confuses the algorithm. This type of error is computed using the following equation

$$\text{Edge detection error} = \frac{|L_{MV} - L_P|}{L_P} \times 100\% \quad (2)$$

2. Panorama generation error in which images are not correctly patched together due to the same colour intensity across the surface texture. This results in difficulty in getting an exact correlation between consecutive frames in a video. A median value of all the matches is used to compute possible correlation, and the value may or may not

Fig. 8 Illustration of upper level gaps (dashed lines) and lower level gaps (solid lines)
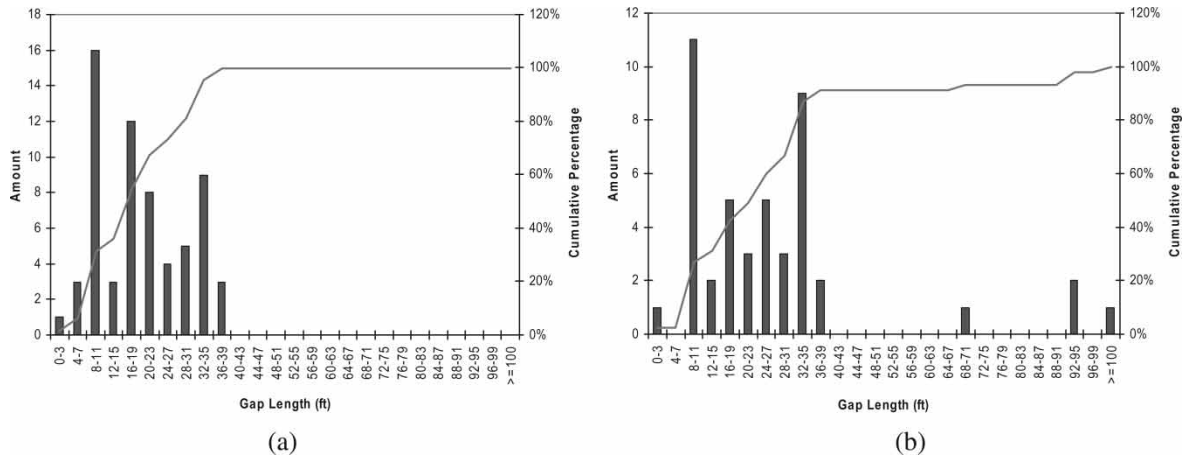
Fig. 9 Frequency distribution of: (a) lower level gaps and (b) upper level gaps in an example train

be the exact estimate of the amount of correlation. Consequently, there are some overlap errors in the panorama generation. Because edge detection is done after the panorama is generated, the output of the gap length may still not be correct even though the edges are correctly identified. This source of error is calculated as follows

$$\text{Panorama generation error} = \frac{|L_P - L|}{L} \times 100\% \quad (3)$$

Videos for ten IM trains with mixed combinations of containers or trailers on well, spine, or flat cars were processed and validated by comparing them to the actual gap lengths (Fig. 10). There was very little difference between the actual and MV results, indicating that the system can successfully detect load

edges in most cases. The average MV edge detection errors for the ten trains analysed was less than 1 per cent for both upper and lower level gaps.

Regarding estimation of panorama-generation error, a reference value was needed to determine the actual length (L) in equation (3). The actual length of loads is standardized [8] and the nominal length is often displayed on their sides so we used this to assess panorama generation error. The average panorama generation error for the ten trains evaluated was less than 4 per cent, ranging from 1.65 to 6.82 per cent (Table 1).

Combining both types of errors, the resultant average error is approximately 5 per cent. If the gap length is less than the critical gap length ($=12$ ft $=3.66$ m), this represents a ± 0.6 ft (0.183 m) difference between the actual and MV output. This is acceptable for the purpose of this technology because the resulting

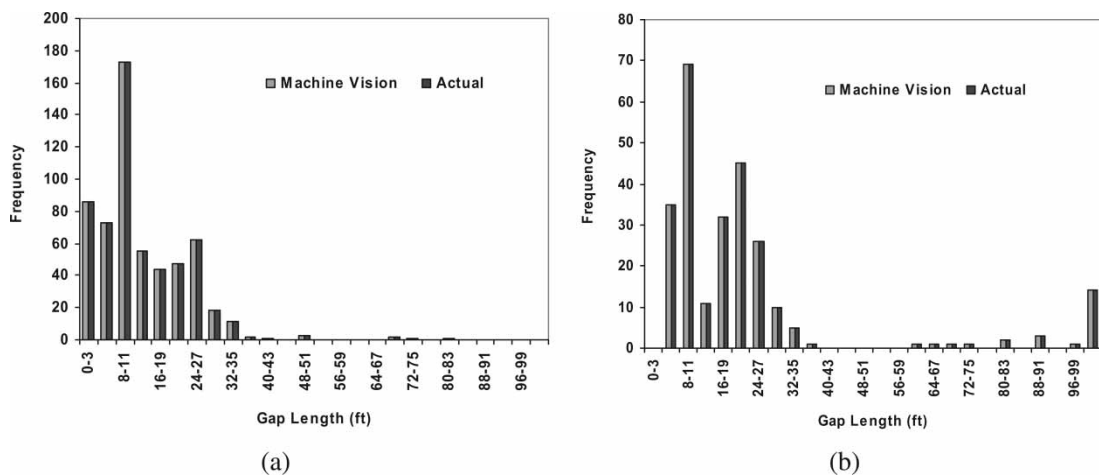**Fig. 10** Frequency diagram of actual train data versus MV data of the: (a) upper level gaps and (b) lower level gaps

**Table 1** Panorama generation error of ten trains evaluated

Train	Date	Panorama generation error (%)
1	6/8/04	3.47
2	6/8/04	1.65
3	8/7/04	2.67
4	9/10/04	3.32
5	9/10/04	2.86
6	9/11/04	6.82
7	9/11/04	4.68
8	9/11/04	2.84
9	9/17/04	2.31
10	9/17/04	4.97
Average		3.56

difference in the aerodynamic coefficient is small. Although the error may be larger for longer gaps (over 12 ft = 3.66 m), this is inconsequential because these gaps exceed the critical gap length and thus the aerodynamic effect is the same (Fig. 2).

4.3.3 Scoring system

The gap histogram shows the distribution of gap lengths in a train regardless of railcar types. Since railcars differ by which IM loads are most efficiently loaded on them, the histogram alone is not sufficient to evaluate the maximum possible efficiency of loading patterns. Hence, a scoring system based on two attributes, aerodynamic coefficient, and slot efficiency, were developed. The aerodynamic coefficient is calculated using the Aerodynamic Subroutine of the AAR TEM (Fig. 11). The IM load information is obtained from the MV output, and railcar type from the AEI tag. The train consist generator can match loads with cars and create a data input of train consists for the Aerodynamic Subroutine. The aerodynamic coefficient is then computed for efficiency evaluation.

This attribute, the aerodynamic coefficient, can be used to estimate fuel consumption with lower values indicating higher fuel efficiency. This coefficient is useful for within train-type comparisons of loading efficiency, but it cannot be used to determine the loading between different types of trains. This is because of constraints imposed by equipment design. For
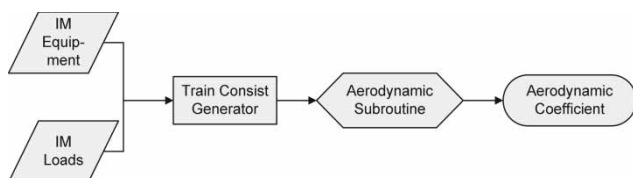
Fig. 11 Flowchart illustrating the process of generating the aerodynamic coefficient used in the scoring system
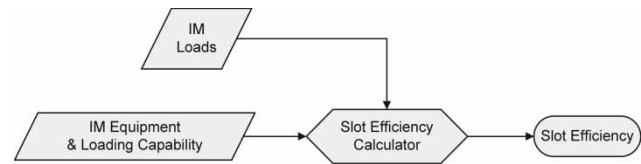
Fig. 12 Flowchart illustrating the process of generating the slot efficiency in the scoring system

example, trains with well cars generally have poorer aerodynamics than trains with spine cars because of the larger gaps due to well car design. Trains loaded with trailers also generally have poorer aerodynamics than trains loaded with containers due to the presence of the hitch, trailer landing gear, and wheels below the floor of the trailer, all of which create additional drag. Hence, when comparing different types of trains, a higher aerodynamic coefficient does not necessarily indicate a poorer loading pattern.

The second attribute, slot efficiency, represents the difference between the actual and ideal loading configuration given the particular set of railcars in the train and the loads available [21]. The IM load information is again obtained from the MV output, and railcar type from the AEI tag. Every slot in each type of railcar has an ideal load that can be determined using the loading capability of each railcar based on data in the universal machine language equipment register (UMLER) database [31]. With the data above as input, slot efficiency is computed based on the percentage of the length of the actual load compared to the length of the ideal load (equation (4)), which is then averaged resulting in the final value for the train (Fig. 12).

The slot efficiency of each slot is calculated as follows

$$\text{slot efficiency} = \frac{\text{length of actual load}}{\text{length of ideal load}} \times 100\% \quad (4)$$

For example, the aerodynamic score of a 45-ft trailer on a 53-ft-slot spine car unit is 85 per cent, whereas placement of a 53-ft trailer on a 53-ft-slot spine car unit generates the lowest aerodynamic resistance and thus the highest score (100 per cent) for this size slot. Slot efficiency is similar to slot utilization except that it also factors in the energy efficiency of the load/slot combination.

5 DISCUSSION

Matching IM loads with cars of an appropriate length to maximize slot efficiency results in improvement in bearing, rolling, and aerodynamic resistances. This can provide greater energy efficiency than maximizing slot utilization alone. If the loads and cars are matched, the aerodynamic benefit ranged from 5 to

36 per cent [**21**]. In an analysis of a typical double stack train on a typical route, fuel consumption was reduced by 0.13 to 0.52 gal/mile (0.306 to 1.223 l/km) depending on the load-and-car combinations being compared. When these amounts are extrapolated to the 800 to 2000 mile (1287 to 3219 km) distances typical of many IM trains, the potential for fuel savings is substantial.

The MV system provides terminal managers feedback on loading performance for trains after they have been loaded. To further assist railroads in fuel savings, a load assignment model was developed to help terminal managers make the best decisions regarding how to load trains so as to maximize their energy efficiency [**32**]. This model is intended to be incorporated into terminal operation software as a decision support tool in the near future.

6   CONCLUSION

A wayside MV system was developed to automatically scan passing trains and assess the aerodynamic efficiency of the loading pattern. The MV system uses an advanced camera that images each container or trailer as trains pass by. MV algorithms are used to analyse these images so as to detect gaps between loads and develop a quantitative index of the loading efficiency of the train.

Combined with the car information from AEI, an index is developed based on the aerodynamic effects of IM load-and-car combination to evaluate slot efficiency. At the macro level, the data collection and analysis system could be deployed to monitor system-wide IM train loading efficiency. At the micro level, it can provide feedback on specific trains originating from particular terminals to help managers create more efficiently loaded trains.

ACKNOWLEDGEMENTS

REFERENCES

1 **Wellington, A. M.** *The economic theory of railway location*, sixth edition, 1900 (John Wiley & Sons, New York).

2 **Association of American Railroads (AAR).** *Railroad facts*. Association of American Railroads, Washington, DC, 2004, 2005, 2006.

3 **International Union of Railways (UIC).** Proceedings of 2nd UIC Railway Energy Efficiency Conference, International Union of Railways, Paris, 2004.

4 **BNSF Railway Company.** Every drop counts in goal to improve fuel efficiency, BNSF News, BNSF Railway Company, 2004.

5 **Stodolski, F.** *Railroad and locomotive technology roadmap*. Report ANL/ESD/02-6, Argonne National Laboratory, Argonne, IL, 2002, available from http://www.transportation.anl.gov/pdfs/RR/261.pdf, accessed 20 February 2003.

6 **Smith, R. A.** How they may contribute to a sustainable future? *Proc. Instn Mech. Engrs, Part F: J. Rail and Rapid Transit*, 2003, **217**(4), 243–248.

7 **Wierderkehr, P.** Environmentally sustainable transport (EST) – driving the economic development? In Proceedings 2nd UIC Railway Energy Efficiency Conference, International Union of Railways, Paris, 2004.

8 **Barkan, C. P. L.** Cost effectiveness of railroad fuel spill prevention using a new locomotive refuelling system. *Transp. Res. D, Trans. Environ.*, 2004, **9**, 251–262.

9 **Gallamore, R. E.** State of the art of intermodal freight transport in the United States. In *Intermodal freight transport in Europe and the United States*, 1998 (Eno Transportation Foundation Inc.).

10 **Muller, G.** *Intermodal freight transportation*, 4th edition, 1999 (Eno Transportation Foundation and Intermodal Association of America, Washington, DC).

11 **Association of American Railroads (AAR).** Proceedings Railroad Energy Technology: The Alternatives, Railway Systems & Management Association, North Field, NJ, 1981.

12 **Association of American Railroads (AAR).** Proceedings Railroad Energy Technology Conference II, Association of American Railroad, Chicago, IL, 1987.

13 **Baker, C. J.** Fact and friction. *Mod. Railw.*, 1984, **41**(425), 86–88.

14 **Smith, M. E.** Economics of reducing train resistance. In Proceedings Railroad Energy Technology Conference II, Association of American Railroad, Chicago, IL, 1987, pp. 269–305.

15 **Davis, W. J. Jr.** Tractive resistance of electric locomotives and cars. *Gen. Electr. Rev.,* 1926, **29**, 685–708.

16 **Gielow, M. A.** and **Furlong, C. F.** *Results of wind tunnel and full-scale tests conducted from 1983 to 1987 in support of The Association of American Railroad's Train Energy Program*, Publication R-685, 1988 (Association of American Railroad, Washington, DC).

17 **Engdahl, R.** *Full-scale rail car testing to determine the effect of position-in-train on aerodynamic resistance*, Publication R-705, 1987 (Association of American Railroad, Washington, DC).

18 **Engdahl, R., Gielow, R. L.,** and **Paul, J. C.** Train resistance – aerodynamics volume I of II intermodal car application. In Proceedings of Railroad Energy Technology Conference II, Association of American Railroad, Washington, DC, 1987, pp. 225–242.

19 **Engdahl, R., Gielow, R. L.,** and **Paul, J. C.** Train resistance – aerodynamics volume II of open top car application. In Proceedings of Railroad Energy Technology Conference II, Association of American Railroad, Washington, DC, 1987, pp. 243–266.

20 **Drish, W. F.** *Train energy model version 2.0 technical manual*, Publication SD-040, 1992 (Association of American Railroads, Washington, DC).

21 **Lai, Y. C.** and **Barkan, C. P. L.** *Options for improving the energy efficiency of intermodal freight trains.* Transportation Research Record 1916, Transportation Research Board, Washington, DC, 2005, pp. 47–55.

22 **Union Pacific Railroad Corporation.** *Intermodal loading guide*, Union Pacific Railroad Corporation, available from http://www.uprr.com/customers/dam-prev/loading/intguide/, accessed 15 July 2004.

23 **BNSF Railway Company.** *Intermodal loading guide,* BNSF Railway Company, 2004.

24 **TTX Company.** *Equipment guide,* TTX Company, 1999.

25 **Optimization Alternatives Ltd. Inc.** *Optimization alternatives' strategic intermodal scheduler.* Optimization Alternatives Ltd. Inc., available from http://www.oax.com/Products/products_oasis.htm, accessed 20 July 2004.

26 **Burriss, C.** Eastbound statistical analysis: slot utilization & mixed cars. In OASIS Users' Conference, Austin, TX, 2003.

27 **Furlong, C. F.** *Aerodynamic subroutine users guide,* Publication R-683, 1988 (Association of American Railroads, Washington, DC).

28 **Hay, W. W.** *Railroad engineering,* second edition, 1982, pp. 69–89 (John Wiley & Sons, New York).

29 **American Railway Engineering and Maintenance-of-Way Association (AREMA).** *Manual for railway engineering,* vol. 2, Train Performance, 2001 (American Railway Engineering and Maintenance-of-Way Association, Landover, MD).

30 **Armstrong, J.** *The railroad: what it is, what it does?,* 1998 (Simmons-Boardman Books, Inc.).

31 **Association of American Railroads (AAR).** *UMLER data specification manual.* Railinc Corporation, 2005, available from http://www.railinc.com/docs/umler_data_spec_manual.pdf, accessed 14 July 2007.

32 **Lai, Y. C., Ouyang, Y., Barkan, C. P. L.,** and **Onal, H.** Optimizing the aerodynamic efficiency of intermodal freight trains with rolling horizon operations, recommended for acceptance. In Proceedings of Transportation Research Board, Transportation Research Board, Washington, DC, 2007.

APPENDIX

Notation

C	aerodynamic coefficient (lbs/(mile/h)^2)
L	gap length of actual train data
L_P	gap length in the panoramic image
L_{MV}	gap length from MV output
R	train resistance (lbs)
R_{Bk}	bearing resistance acting on vehicle k (lbs)
R_{Rk}	rolling resistance acting on vehicle k (lbs)
V	train speed (mile/h)